

# DEVELOPING NOVEL BIOPHYSICAL TOOLS TO OVERCOME THE CURRENT ANTIBIOTIC FAILURE

University of Exeter, Exeter, U.K

## Abstract

*Novel advances in microfluidic technology, such as the so-called mother-machine device, have for the first-time enabled researchers to quantify single-cell responses under precise environmental controls; opening up a range of potential avenues for microbiological research. Despite this, image analysis of the large quantities of data produced has remained a major bottleneck. Here, we present the ilastik mother-machine python (iMMPY) protocol version 2.1 - a semi-supervised machine-learning based protocol enabling rapid analysis of mother-machine imagery. iMMPY version 2.1 facilitates the extraction of up to 15 different experimental variables, recording an extremely low error rate of just 0.02% against our test dataset. Due to the tailored use of machine-learning, we believe our protocol can be suitable for a wide range of mother-machine based experimentation. We actively demonstrate the utility of the protocol by analysing antibiotic accumulation trials across six fluorescently labeled drugs, establishing a ranking of antibiotic permeability and highlighting significance in the ability of tachyplysein to permeate the gram-negative barrier. Analysis of antibiotic trials with polymyxin B also displayed significant increases in antibiotic accumulation, indicating prospective avenues for further research.*

## I. INTRODUCTION

Antimicrobial resistance (AMR), remains one of the greatest threats we face today as a global community, with predictions estimating over 10 million AMR related deaths annually by 2050<sup>1</sup>. Of particular concern are gram-negative bacterial infections. Facilitating a distinctive double-membrane responsible for resistance to a wide range of antibiotics including  $\beta$ -lactams, quinolones and colistins<sup>2–5</sup>, gram-negative bacterial infections have dramatically increased in recent years across all parts of the world, posing an increasingly serious challenge for healthcare professionals. Despite the ever-prevalent threat, the discovery and development of novel antibiotic drugs has declined considerably in recent decades<sup>6</sup>. As such, the development of innovative approaches toward the research & development of antibiotics are of crucial importance in order to overcome the impending antibiotic failure.

Recent advances in microfluidic technology, culminating in novel microfluidic chips such as the so-called mother-machine (MM) device<sup>7</sup>, have brought about an unprecedented level of access towards understanding and manipulating micro-scale phenomena. By capturing and growing individual mother cells in micro-fabricated geometries, microfluidic techniques bypass several limitations of population averaged studies<sup>8</sup>, uniquely granting scientists the ability to investigate biological events

with single-cell resolution and precise control over environmental conditions. When coupled with time-lapse and fluorescence microscopy, referred to as the mother-machine setup, high fidelity data for individual cells can be acquired over hundreds of generations. Because of its potential to investigate a variety of novel research questions, the mother-machine setup has seen widespread adoption in recent years promoting investigations into population heterogeneity<sup>9</sup>, growth regulation<sup>10</sup>, and of course antibiotic resistance and accumulation<sup>11–12</sup> to name a few.

While great strides in research capability have been made, our ability to analyse the vast quantities of imagery remains a major bottleneck. With single frames containing up to 100 bacteria and imaged regions often containing hundreds of frames per dataset, traditional manual methods of analysis have become unfeasibly time-consuming without sacrificing large proportions of data. While several research groups have come up with various automated<sup>13–15</sup> and semi-automated<sup>16–17</sup> analysis tools to alleviate this problem, such software have proven highly specialized and therefore, applicable to the wider community only under a narrow range of experimental conditions.

One such tool known as iMMPY (ilastik mother-machine python), initially developed by 4th year natural sciences students at the University of Exeter for fluorescence based research, proposes a promising founda-

tion for the development of a truly multipurpose, and therefore, widely applicable research tool for MM based experimentation. Utilisation of the machine learning software, ilastik, in theory, allows for a comprehensive range of uses granting a unique adoption point compared to other MM tools. Such an approach further allows for special consideration of frames featuring high levels of noise or variation in focus, blurring otherwise well-defined features – a common issue in mother-machine imagery. Despite great potential, iMMPY has remained in a prototypical state owing to several key deficiencies that can be summarised below:

- 1 - Unrefined methodology:** inefficient algorithm training and mask creation processes result in excessive computational volumes and frequent crashing.
- 2 - Dysfunctional data export:** data output limited to graphs and therefore highly niche use-cases.
- 3 - No integration of time-codes:** uses frame number, severely restricting usefulness of the generated graphs.
- 4 - Non-trivial issues:** e.g. non-existent ‘ghost cell’ lineages, random errors and little support for Mac OS.
- 5 - Designed for use with fluorescence imagery:** limited utilisation for wider scale research.

In this paper, we present iMMPY version 2.1, an overhauled and widely applicable MM image analysis protocol based upon the framework of iMMPY. We implement a refined methodology, overcoming previous limitations, with an extended array of analysis features including tracking IDs, allowing researchers to trace exported data back to imaged cells. We demonstrate an exceptionally low error rate, whilst facilitating greater utility on everyday hardware. We further demonstrate the value of iMMPY V2.1 by analysing experimental data primarily gathered from the Pagliara group for antibiotic accumulation trials across six antibiotics; tachyplesin, roxithromycin, oxazolidinone, trimethoprim, ciprofloxacin & vancomycin, ranking their ability to permeate the *E. coli* double membrane. We analyse trials with polymyxin B, a promising membrane permeabilizing agent, and *P. aeruginosa* - a clinically relevant bacterium listed as priority 1 for antibiotic resistance by the World Health Organisation (WHO).<sup>18</sup>

## II. EXPERIMENTAL METHODS

### *Antibiotic Conjugates:*

Antibiotic conjugates utilised in this study feature a nitrobenzofurazan (NBD) fluorophore recognition group, acquired from Dr Mark Blaskovich, University of Queensland.<sup>19</sup>

### *Bacterial Cell Culture:*

Bacterial cultures were prepared by picking a single colony of *E. coli* (BW25113) or *P. aeruginosa* (PA14) from a streak plate and growing it in 100 ml fresh LB medium (10g l<sup>-1</sup> tryptone, 5g l<sup>-1</sup> yeast extract, and 0.5g l<sup>-1</sup> NaCl) in a shaking incubator at 200 rpm and 37°C for a duration of approximately 17h before usage.

### *Microfluidic Chip and Cell Loading:*

The mother machine microfluidic chips are comprised of polydimethylsiloxane (PDMS), constituting a main “feeding channel” (25 um in height and 100 um in width) and thousands of “growth channels” (25 um in length and 1.4 um in height and width). The PDMS chips were carefully punched with a 1.5 mm biopsy punch, creating fluidic inlets and outlets as depicted in Fig 1(a). The devices were bound to a type 1 coverslip via air plasma treatment (30W plasma power with an exposure time of 10s) and held at 70°C for an additional 5 min to increase adhesion. The chips were flushed with ethanol to sterilise the device before being filled with 50 mg ml<sup>-1</sup> of bovine serum albumin (BSA) enabling passivation of the internal circuit thus, reducing cellular adhesion toward the internal surfaces.

The overnight cell culture was resuspended to an optical density of 50 (at 595 nm). An aliquot of this culture solution was injected in the mother-machine device and incubated at 37°C for 20 min enabling cells to enter the microfluidic growth channels. For the exponential growth phase experiments, chips were further flushed with LB (100 µl h<sup>-1</sup>) for 3 hours causing the cells to enter the exponential growth phase. A 1g l<sup>-1</sup> glucose media was then flushed through the device (at 300 µl h<sup>-1</sup>) for 10 min to wash out the LB while preventing cells from starving. The antibiotic-fluorophore conjugates, as mentioned above, were then perfused through the device at a rate of 100 µl h<sup>-1</sup> with a concentration of 46 µg ml<sup>-1</sup> unless otherwise stated.

### *Microscopy Setup & Imaging:*

All experimentation was undertaken using an Olympus IX73 epifluorescence microscope with an LED light source at the 365 nm excitation wavelength. The LED was triggered by the camera, ensuring cells were only exposed to excitation light during image acquisition. The time-lapse images were taken at regular intervals throughout the duration of each experiment in complimentary brightfield and fluorescence pairs. An image exposure of 30ms for brightfield and fluorescent images was utilised. A heating stage was additionally used to maintain cells at the optimum temperature of 37°C.

### **Machine Learning & Image Analysis**

A detailed protocol and image optimisation guide can be downloaded alongside the iMMPY V2.1 python script at: [github.com/Aaron-S-Walker/iMMPY-Protocol.git](https://github.com/Aaron-S-Walker/iMMPY-Protocol.git). See appendix for further information.

#### **Stage One: Pixel classification:**

As specified in the protocol, image pairs were first filtered for sudden variations in contrast or loss or focus. The brightfield image stacks were imported into an ilastik pixel classification project for algorithm training. Using a “background” colour, yellow by convention, points of interest such as channel numbers, empty channels and the feeding channel were discreetly marked using a size 3 classifier brush. Using an “object” colour, conventionally blue, cells were covered over and thinly separated using the background colour – see Fig 1(c). This process was repeated until a minimum of 100 bacteria were classified.

#### **Stage Two: Tracking with learning:**

The pixel classification exports were imported into a new tracking with learning project in ilastik. A prediction threshold of 70% was applied with an artificial smoothing ratio of 1:1.4 leading to cell identification as depicted in Fig 1(d). A minimum size filter of 30 pixels was applied to remove prediction noise. Object and division classification with learning was carried out, ensuring all cells and divisions were correctly identified. Export of the tracking with learning project produced a refined binary classification map as shown in Fig 1(e).

#### **Stage Three: Channel Masks:**

Channel masks were created using the open-source software GIMP with third party plugins to streamline the masking process. A series of uniform rectangular channel masks were implemented over desired growth channels, enabling the analysis script to ignore detections outside of these regions of interest. The individual masks from the initial frame were linked and reused for each successive frame, making subtle adjustments to account for slight variations between frames.

#### **Stage Four: Image Analysis:**

The iMMPY V2.1 python script takes up to four inputs: brightfield & fluorescence images, the ilastik-classification masks and channel masks. Using the easily navigable interface, users can select the level of output detail, corresponding to individual variables which are exportable as separate .CSV file types. Complimentary to the .CSV files, iMMPY produces a graphical representation for each selected variable enabling the user to visualise the mean and individual cell data without additional data handling.

### **III. RESULTS**

Version 2.1 of the iMMPY analysis script currently facilitates the extraction of up to 15 variables ranging from resultant fluorescence to cellular eccentricity exportable as individual .CSV file types. While the iMMPY protocol and Python script were initially designed to run with brightfield-fluorescence image pairs, version 2.1 provides functionality without the dependence of fluorescence images, enabling wider scale applicability across mother-machine based imaging experiments. New implementations include the automatic extraction of image time codes, included in the exported files as a header, and the introduction of unique identification (UID) and channel identification (CID) numbers, included as a left sided header. These additions enable researchers to visually locate cells with data of special interest, or vice versa, offering particular value for long-duration studies e.g. investigations into cellular senescence or persistence.

A significant improvement in the version 2.1 python script was the elimination of ‘ghost cell’ lineages which were a major limiting factor contributing to error. As demonstrated in our test set, a total of 77 cell lineages were identified via manual analysis, with 78 identified via iMMPY V2.1 and 134 via iMMPY V1.0 (including ghost lineages), see Fig 2(a-c). An overall error rate of 8.2% was previously reported against the test dataset for iMMPY V1.0, however, when accounting for ghost cell lineages, highlighted red in Fig 2(b), the overall error rate is shown to be approximately 42.6%.

#### **iMMPY V2.1 computational performance:**

With iMMPY version 2.1 we introduce notable accuracy, resource-efficiency and functionality improvements to the protocol and analysis script. We were able to analyse the test dataset in under 30 minutes, consisting of approx. 28 minutes of manual work (algorithm training and data preparation) and under one minute of computation time - facilitating an overall error rate of 0.02% (1 tracking error out of 4389 total measurements). An average iteration rate of 1.54 frames per second was recorded, equating to 112 measurements per second (or 8.9 msec per measurement) using an i7-6700K CPU with 16GB RAM. For comparison, manual analysis of the test dataset took on average 25 seconds per measurement, or 32 minutes per frame, with a total of 30 hours of manual work required for completion.

#### **Antibiotic accumulation analysis:**

A total of 3,717 cells were tracked across the 10 experiments analysed in this paper – totalling over 2,750,000 measurements. While this paper showcases

Table I: Antibiotic permeability

This table provides a ranking of antibiotic permeability capability against the gram-negative bacterial double membrane.

Drug	Bacterium	Growth Phase	No. Cells	T <sub>0</sub> (min)	T <sub>1/2</sub> (min)	T <sub>Max</sub> (min)	Max Fluorescence (a.u)
Tachypleasin	<i>E. coli</i>	Exponential	78	3.34	27.5	124	3364 ± 363
Oxazolidinone	<i>E. coli</i>	Exponential	355	4.08	24.0	154	756 ± 71
Roxithromycin	<i>E. coli</i>	Exponential	575	8.45	132	158	631 ± 645
Trimethoprim	<i>E. coli</i>	Exponential	272	4.78	75.2	156	343 ± 40
Ciprofloxacin	<i>E. coli</i>	Exponential	408	11.44	72.7	142	262 ± 57
Vancomycin	<i>E. coli</i>	Exponential	327	87	111	157	57 ± 89
Roxithromycin + PolyB	<i>E. coli</i>	Exponential	388	5.7	74.5	143	883 ± 83
Vancomycin + PolyB	<i>E. coli</i>	Exponential	569	119	159.7	159	222 ± 238
Ciprofloxacin	<i>P. aeruginosa</i>	Exponential	178	84.0	121	154	63 ± 24
Ciprofloxacin	<i>P. aeruginosa</i>	Stationary	567	-	112	151	7.5 ± 9

fluorescence data, all 15 variables were acquired for each of the 73 datasets analysed, providing potentially useful data for further publications. The key numerical data for this paper is provided above in table 1, with individual accumulation profiles shown in Fig 3.

For exposure durations of up to 160 min, tachypleasin demonstrated the greatest permeability against the gram-negative barrier. Peak fluorescence for tachypleasin was recorded to be 3364±363 a.u. (after 124 min exposure), demonstrating an antibiotic accumulation over 4-fold that of the next highest – oxazolidinone (756±71 a.u. recorded after 154min of exposure). Expectedly, vancomycin recorded the lowest peak antibiotic accumulation with a max fluorescence of 57±89 a.u. (after 157 min exposure). Looking at the initial uptake times, T<sub>0</sub>, defined as the point at which fluorescence exceeds the background noise threshold of 20 a.u., we see a similar trend in accumulation onset as we do for max accumulation with onset times of 3.34, 4.08 and 87 min for tachypleasin, oxazolidinone and vancomycin, respectively. Notably, however, we identify an antibiotic accumulation onset for trimethoprim of 4.78 min, compared to 8.45 min recorded for roxithromycin, despite facilitating max accumulations of 343±40 and 631±645, respectively.

Experimental data for roxithromycin and vancomycin accumulation against *E. coli*, tested with and without polymyxin B, display a notable increase in accumulation for both antibiotics while treated with polymyxin B – see Fig 4(d-e). Undertaking a Kolmogorov–Smirnov test we find a statistically significant increase in antibiotic accumulation when these drugs are treated with polymyxin B, facilitating a p-value of <0.0001 for both the roxithromycin and vancomycin trials.

*P. aeruginosa* trials, tested in two different growth phases against the antibiotic ciprofloxacin recorded a

significant increase in permeability (p-value<0.0001) when treated in exponential compared to stationary growth phases - see Fig 4(f). A significant decrease in permeability is further seen when comparing the exponential phase accumulation profiles of *E. coli* and *P. aeruginosa* against ciprofloxacin (p-value<0.0001).

#### IV. DISCUSSION

As detailed in the results section, we believe the updated iMMPY V2.1 protocol has the potential to be an invaluable analysis tool for mother-machine research. Version 2.1 provides researchers with a more refined and resource-efficient approach to algorithm training, lending an enhanced level of accessibility to researchers without specialised hardware e.g. laptops or desktop PCs. Our ‘discreet’ approach substantially reduces the computational volume required, demanding appreciably less user input to attain good results compared to previous methods. This considerably improved the efficiency of algorithm training, going from up to 12 min computation per iteration to near real-time feedback during pixel classification. iMMPY V2.1 further implements the ability to successfully extract, combine and easily interpret data from across many different imaging regions, a previously dysfunctional aspect limiting the iMMPY protocol’s utility. As each mother-machine device accommodates thousands of microfluidic growth channels, such implementations enable analysis to be carried out across a significantly larger proportion of the microfluidic device’s trackable cell capacity - leaving less unutilised data per experiment.

In contrast to manual analysis, which typically places a rectangular box over each cell to extract information, the use of machine learning, generating probability maps, facilitates a large jump in measurement precision. While both methods take averaged measurements for fluorescence over a fixed area, the use of

pixel prediction maps serve to alleviate background regions otherwise included in manual measurements. This acts to reduce systematic error in measurements while further enabling accurate extraction of variables such as perimeter and cellular eccentricity that are near to unfeasible manually.

Unlike the majority of mother-machine analysis tools, iMMPY is a semi-supervised protocol. Fully automated approaches such as those utilised in DeLTA,<sup>13</sup> Molyso<sup>14</sup> and BACMMAN<sup>15</sup> train algorithms via a single large training set, the results of which are tested then applied to all future datasets. While this is the conventional approach, one drawback to such a method is comparatively weaker algorithm generalisation leading to increased segmentation error in unseen datasets.<sup>20</sup> To address this problem, we conduct algorithm training for each individual dataset to account for any unique or isolated considerations. Inclusion of an 'object classification with learning' step enables the user to clarify segmentation events across the dataset. In theory, this facilitates a 0.00% segmentation error rate compared to manual analysis. However, such implementations do not protect against human error. We note a comparatively large improvement in overall error rate at 0.02% compared to the leading 1.07% of DeLTA, however, further trials with more expansive datasets are needed.

While iMMPY V2.1 offers comparatively large improvements in accuracy compared to other mother-machine tools, this comes at an expense of additional time required for data preparation and dataset training. For this reason we find our protocol to be most effective for research generating datasets with up to 1000 frames. Despite such recommendation, iMMPY version 2.1 has quickly proven itself to be a useful tool for a variety of mother-machine based experimentation across the University of Exeter's Stretham and Cornwall campuses, currently in active use by over a dozen researchers ranging from undergraduates to doctoral students.

Within the timescales investigated, our data against *E. coli* indicates a notable significance in the ability of tachyplesin to permeate the gram-negative double membrane, supporting literature indicating tachyplesin's ability to permeabilize the outer membrane and compromise cell membrane integrity.<sup>21–22</sup>

Trials with roxithromycin and vancomycin, ordinarily ineffective against the gram-negative barrier, demonstrate the potential of polymyxin B treatments for permeabilising the outer membrane and significantly increasing antibiotic accumulation. Unfortunately, there are a limited number of studies investigating the use of

polymyxin B for the treatment of gram-negative and multi-drug resistant bacteria,<sup>23–25</sup> the majority of such offer limited use due to small sample sizes.

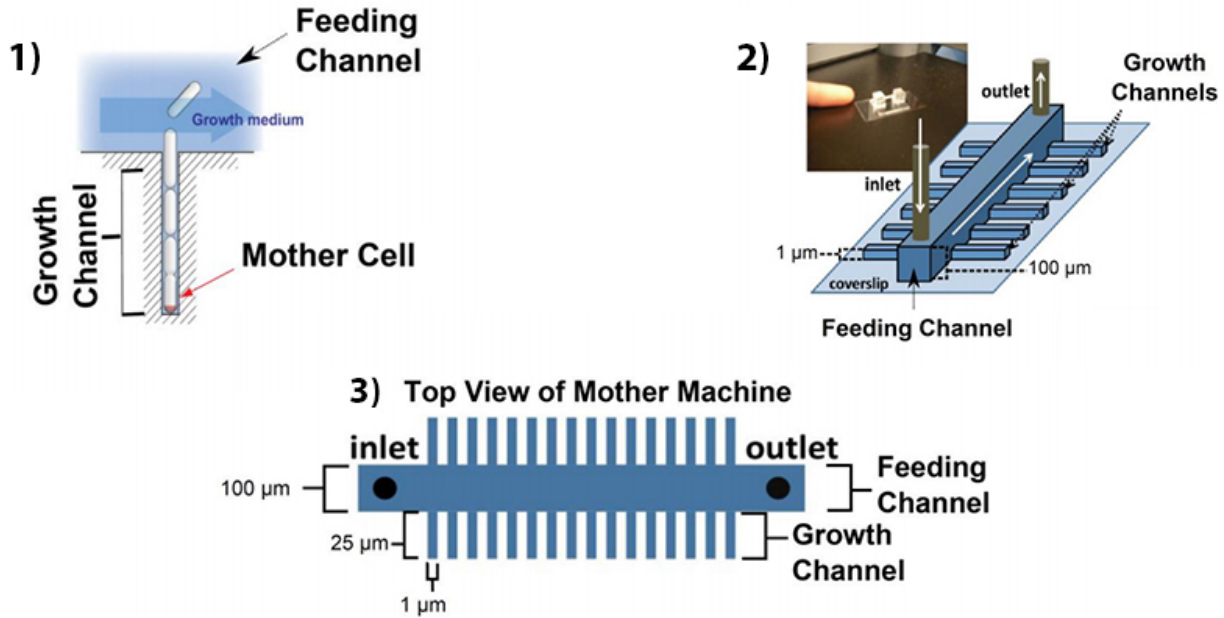
Our experimental data additionally encompassed antibiotic accumulation trials with *P. aeruginosa*, listed as one of three priority 1 strains facilitating critical antibiotic resistance. While the mother-machine and its analysis software are primarily tailored for *E. coli* based research, our trials with *P. aeruginosa* demonstrate the unique potential of the iMMPY V2.1 protocol to re-train, track and analyse a wide variety of biological cell types other than *E. coli*. *P. aeruginosa* trials with ciprofloxacin showed low levels of NBD-fluorescence compared to *E. coli* trials, attributable to a lower outer membrane permeability, contributing to its acquired resistance to all known antibiotic classes.<sup>26</sup> Furthermore, our studies illustrate higher permeability during the exponential versus stationary phase, corroborating recent publication undertaken on *E. coli*.<sup>27</sup>

## V. CONCLUSION

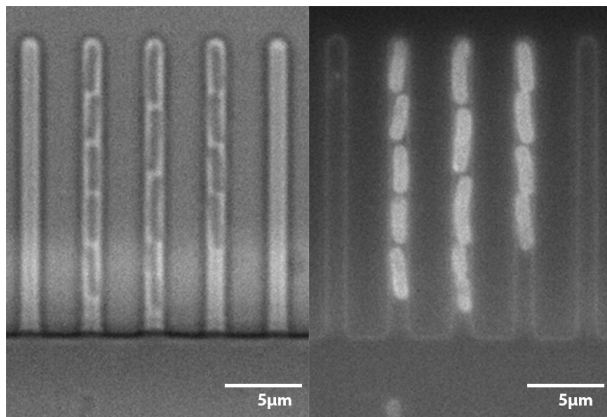
In iMMPY version 2.1, we present what we believe to be a functionally complete and widely applicable semi-supervised machine-learning protocol, enabling rapid analysis of time-lapse imagery. We introduce a 'discreet' approach towards algorithm training, requiring less time and computation compared to previous methods, demonstrating an overall error rate of just 0.02% against our test dataset. By re-training machine learning algorithms for each dataset, our protocol is unique in its inherent ability to analyse biological cell types other than *E. coli*. While intended for use with the mother-machine setup, with minor adjustments the iMMPY protocol could be utilised with a range of different experimental setups.

In demonstrating the analysis capabilities of iMMPY, this paper acts to better inform scientists of potential areas for future research, development and usage of antibiotics. We present a ranking of six antibiotics based on their ability to permeate the gram-negative double membrane, highlighting significance in tachyplesin. Our experimental data signifies polymyxin B as a promising avenue for treatment, while illustrating an increased permeability of *P. aeruginosa* to ciprofloxacin during the exponential versus stationary growth phase.

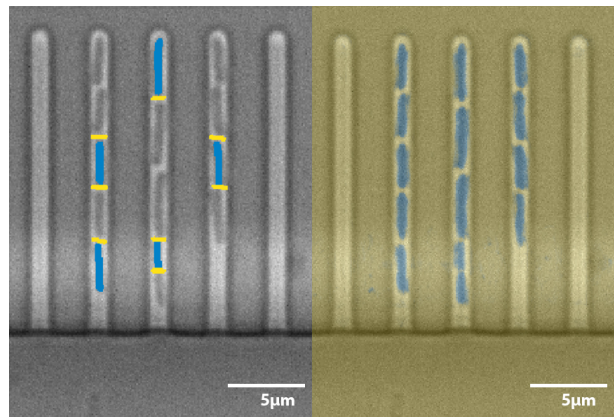
Using the machine learning techniques detailed in this paper, and others similar to it, we hope this study will encourage researchers to use our findings as a template for further antibiotic investigation and innovation.



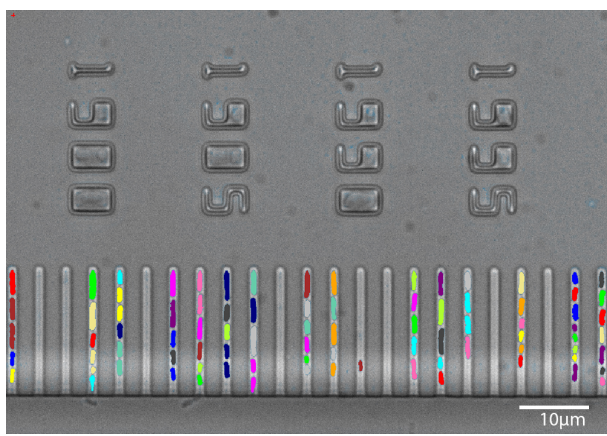
(a) Diagram illustrating the mother machine microfluidic chip layout - Schwall et al.<sup>28</sup>



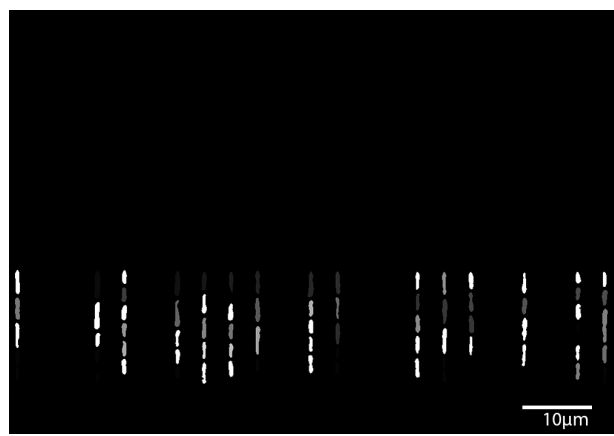
(b) Initial brightfield and fluorescence images.



(c) Pixel classification and pixel prediction map.

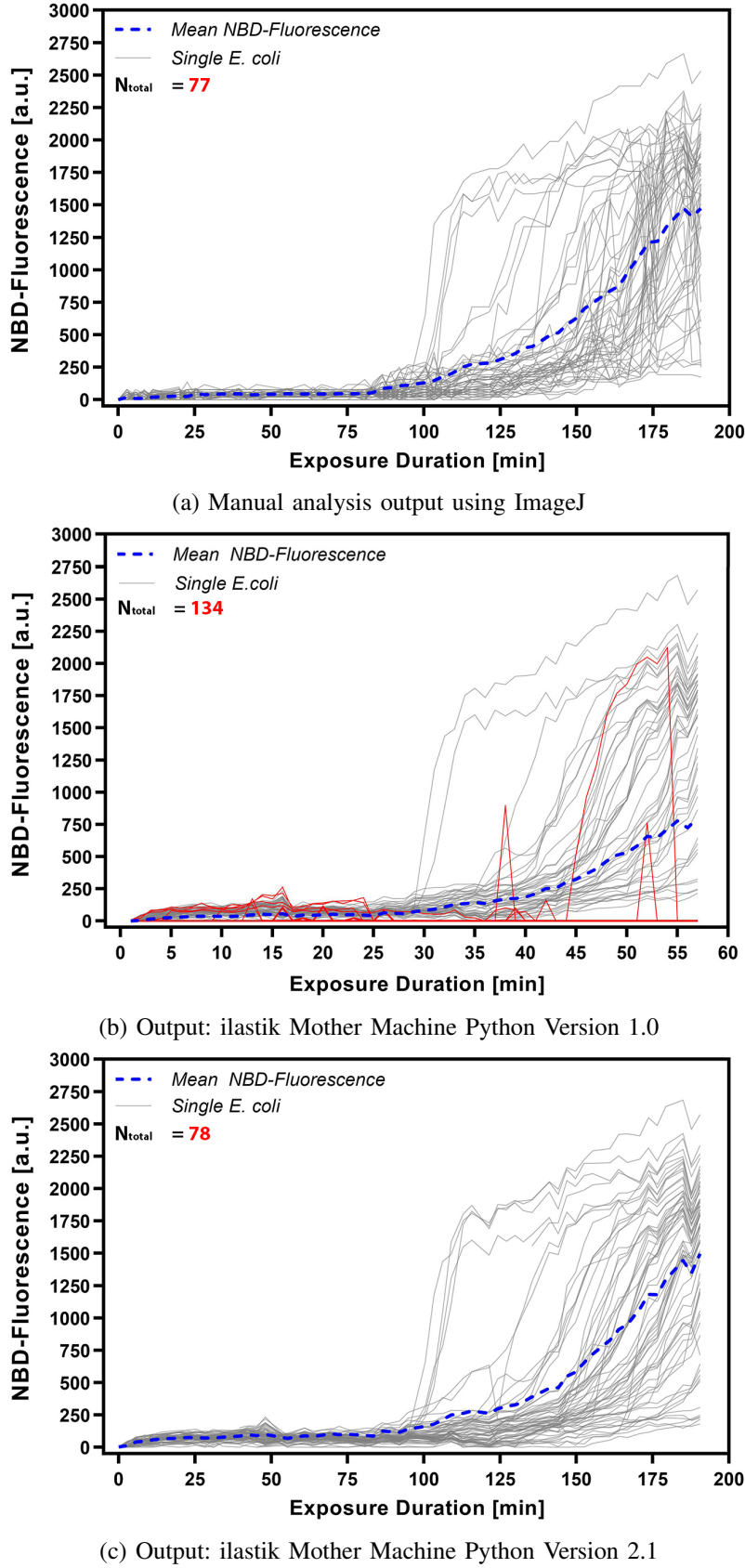


(d) Object classification of pixel prediction map.

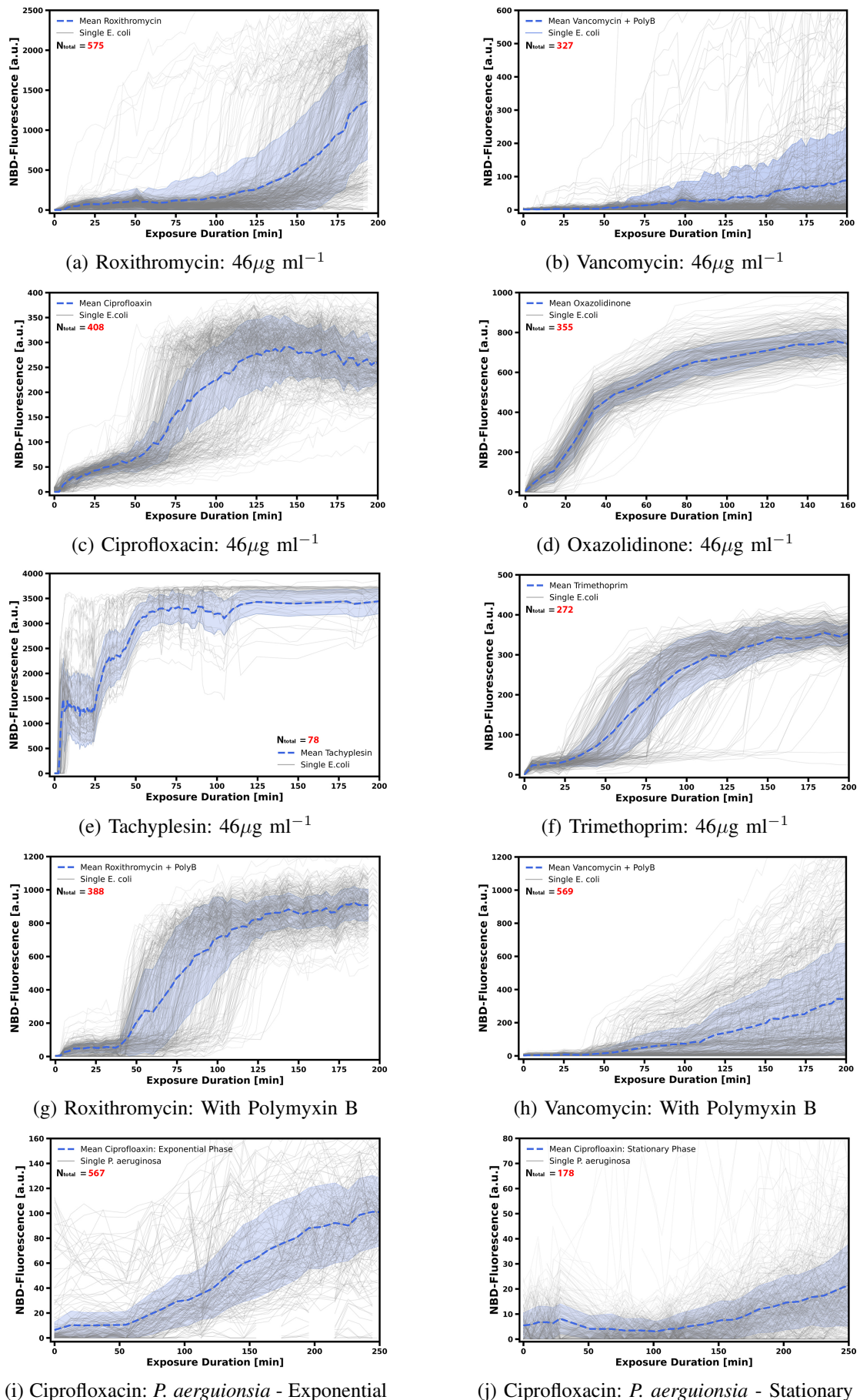


(e) ilastik generated classification mask.

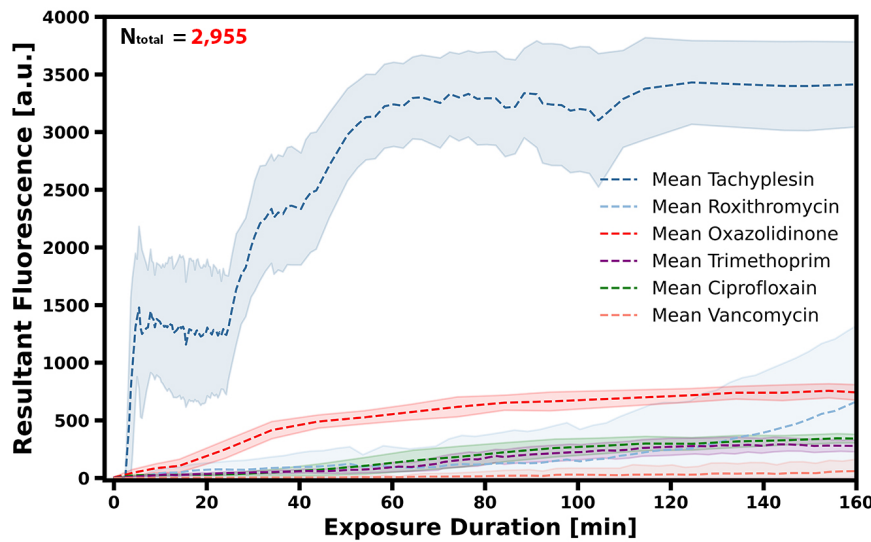
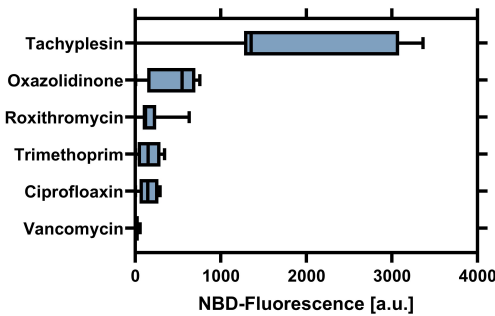
**Figure 1:** Overview of the mother-machine experimental setup and iMMPY protocol, consisting of (a) an illustration of the microfluidic device and (b-e) visualisations from key stages during the iMMPY protocol's algorithm training process.



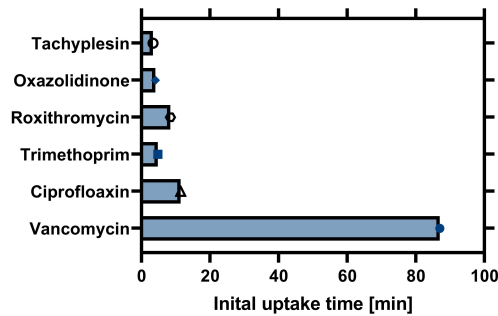
**Figure 2:** Comparison of test dataset outputs via a) manual analysis using ImageJ, b) machine learning analysis using the prototypical version 1.0 of iMMPY and c) machine learning analysis using the upgraded iMMPY version 2.1. Note that single *E. coli* highlighted in red represent erroneous traces (ghost lineages and cells where tracking output is lost for a significant number of frames due to segmentation error).



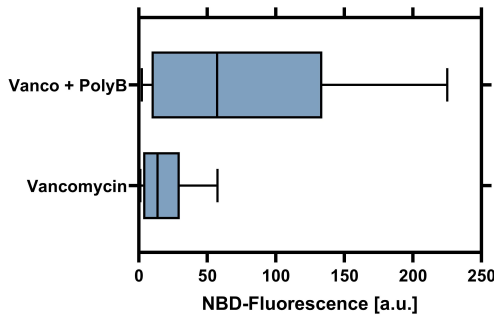
**Figure 3:** Individual antibiotic accumulation profiles across the 10 experiments.

(a) Antibiotic accumulation profiles against *E. coli* for the six drugs tested.

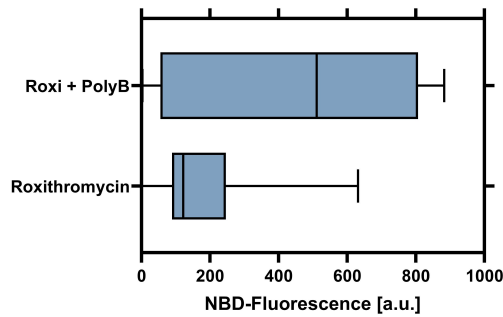
(b) Accumulation across the six drugs tested



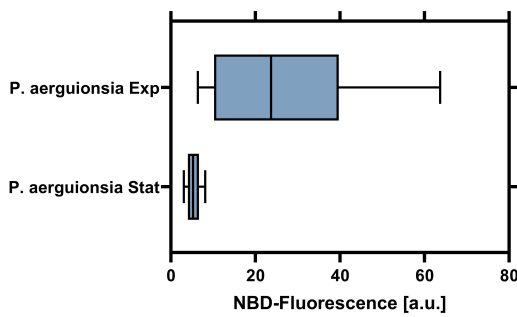
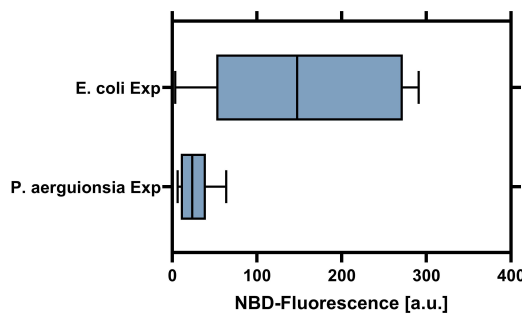
(c) Initial time of antibiotic uptake (To)



(d) Roxithromycin: Polymyxin B trials



(e) Vancomycin: Polymyxin B trials

(f) Ciprofloxacin: *P. aeruginosa* phase uptakes(g) Ciprofloxacin: *E. coli* vs *P. aeruginosa* uptakes**Figure 4:** Comparative antibiotic accumulation plots.

## ACKNOWLEDGMENTS

I would like to thank Dr Stefano Pagliara and Louis Clement-Harris for their continued support over the duration of this project.

## APPENDIX

- In addition to the iMMPY protocol and python analysis script, a tutorial video was recorded to give new researchers an in-depth walk through of the protocol steps. Please contact Dr Stefano Pagliara to gain access to this training resource.
- Further development of the iMMPY protocol has been planned to take place over the course of summer 2021.

## REFERENCES

- [1] O'Neill J. "Review on Antimicrobial Resistance Antimicrobial Resistance: Tackling a crisis for the health and wealth of nations." London: Review on Antimicrobial Resistance; 2014. [cited 2021 March 1]
- [2] Pitout JD, Sanders CC, Sanders WE Jr. "Antimicrobial resistance with focus on beta-lactam resistance in gram-negative bacilli." Am J Med. 1997 Jul;103(1):51-9. doi:10.1016/s0002-9343(97)00044-2.
- [3] Hooper, David C, and George A Jacoby. "Mechanisms of drug resistance: quinolone resistance." Annals of the New York Academy of Sciences. Vol. 1354,1 (2015): 12-31. doi:10.1111/nyas.12830
- [4] Lee, Ji-Young et al. "Preservation of Acquired Colistin Resistance in Gram-Negative Bacteria." Antimicrobial agents and chemotherapy. Vol. 60,1 609-12. 12 Oct. 2015, doi:10.1128/AAC.01574-15
- [5] Ohta, M et al. "Mechanisms of antibacterial action of tachyplesins and polyphemusins, a group of antimicrobial peptides isolated from horseshoe crab hemocytes." Antimicrobial agents and chemotherapy vol. 36,7 (1992): 1460-5. doi:10.1128/aac.36.7.1460
- [6] Zaman, SB, Hussain MA, Nyse R, Mehta V, Mamun KT, Hossain N et al. "A Review on Antibiotic Resistance: Alarm Bells are Ringing." Cureus. Vol 9. Issue 6: e1403. 28 Jun, (2017). doi:10.7759/cureus.1403
- [7] P. Wang, L. Robert et al "Robust Growth of Escherichia coli" Current Biology. Vol 20. Issue: 12: 1099-1103. (2010). <https://doi.org/10.1016/j.cub.2010.04.045>
- [8] Dai, Jing et al. "Microfluidics for Antibiotic Susceptibility and Toxicity Testing." Bioengineering (Basel, Switzerland). Vol 3. Issue 4: 25. 9 Oct, (2016). <https://doi:10.3390/bioengineering3040025>
- [9] Vindenes, Yngvild et al. "Individual heterogeneity in vital parameters and demographic stochasticity." The American naturalist vol. 171,4 (2008): 455-67. doi:10.1086/528965
- [10] Somenath Bakshi, Emanuele Leoncini et al. "Dynamic Regulation of Growth and Physiology of Microbes under Complex Changing Conditions" bioRxiv. 006403. 03.27.2020. doi: <https://doi.org/10.1101/2020.03.27.006403>.

- [11] Cama . J, Pagliara .S et al. “Single-cell microfluidics facilitates the rapid quantification of antibiotic accumulation in Gram-negative bacteria” Lab on a Chip. Vol 20, 2765-2775. 2020. doi.org/10.1039/D0LC00242A
- [12] Arnoldini, Markus et al. “Bistable expression of virulence genes in salmonella leads to the formation of an antibiotic-tolerant subpopulation.” PLoS biology vol. 12,8 e1001928. 19 Aug. 2014, doi:10.1371/journal.pbio.1001928
- [13] Lugagne, Jean-Baptiste et al. “DeLTA: Automated cell segmentation, tracking, and lineage reconstruction using deep learning.” PLoS computational biology vol. 16,4 e1007673. 13 Apr. 2020, doi:10.1371/journal.pcbi.1007673
- [14] Sachs, Christian Carsten et al. “Image-Based Single Cell Profiling: High-Throughput Processing of Mother Machine Experiments.” PloS one vol. 11,9 e0163453. 23 Sep. 2016, doi:10.1371/journal.pone.0163453
- [15] Ollion, Jean et al. “High-throughput detection and tracking of cells and intracellular spots in mother machine experiments.” Nature protocols vol. 14,11 (2019): 3144-3161. doi:10.1038/s41596-019-0216-9
- [16] Kaiser, M., Jug, F., Julou, T. et al. “Monitoring single-cell gene regulation under dynamically controllable conditions with integrated microfluidics and software.” Nat Commun. 9, 212 (2018). <https://doi.org/10.1038/s41467-017-02505-0>
- [17] Divya Ganapathi Sankaran, Alexander J. et al. “A semi-automated machine learning-aided approach to quantitative analysis of centrosomes and microtubule organization” Journal of Cell Science 133: 2020. doi: 10.1242/jcs.243543
- [18] Tacconelli .E et al. “Global Priority List Of Antibiotic-resistant Bacteria To Guide Research, Discovery, and Development Of New Antibiotics” World Health Organisation. 2017. <https://www.who.int/medicines/publications>
- [19] Stone, M Rhia L et al. “Fluorescent Antibiotics: New Research Tools to Fight Antibiotic Resistance.” Trends in biotechnology. Vol. 36,5 (2018): 523-536. doi:10.1016/j.tibtech.2018.01.004
- [20] Dexter, Gregory P et al. “Generalization of Machine Learning Approaches to Identify Notifiable Conditions from a Statewide Health Information Exchange.” AMIA Joint Summits on Translational Science. AMIA Joint Summits on Translational Science vol. 2020 152-161. 30 May. 2020
- [21] Matsuzaki, K et al. “Interactions of an antimicrobial peptide, tachyplesin I, with lipid membranes.” Biochimica et biophysica acta. Vol. 1070,1 (1991): 259-64. doi:10.1016/0005-2736(91)90173-6
- [22] Hong, Jun et al. “Mechanism of tachyplesin I injury to bacterial membranes and intracellular enzymes, determined by laser confocal scanning microscopy and flow cytometry.” Microbiological research vol. 170 (2015): 69-77. doi:10.1016/j.micres.2014.08.012
- [23] Laurent Poirel, Aurélie Jayol, Patrice Nordmann. “Polymyxins: Antibacterial Activity, Susceptibility Testing, and Resistance Mechanisms Encoded by Plasmids or Chromosomes” Clinical Microbiology Reviews. Vol.30, (2), 557-596. 2017. DOI: 10.1128/CMR.00064-16
- [24] Avedissian, Sean N et al. “A Review of the Clinical Pharmacokinetics of Polymyxin B.” Antibiotics (Basel, Switzerland) vol. 8,1 31. 22 Mar. 2019, doi:10.3390/antibiotics8010031
- [25] Zavascki, Alexandre Prehn et al. “Polymyxin B for the treatment of multidrug-resistant pathogens: a critical review.” The Journal of antimicrobial chemotherapy vol. 60,6 (2007): 1206-15. doi:10.1093/jac/dkm357
- [26] David M. Livermore. “Multiple Mechanisms of Antimicrobial Resistance in *Pseudomonas aeruginosa*: Our Worst Nightmare?” Clinical Infectious Diseases, Volume 34, Issue 5, 1 March 2002, Pages 634–640, doi.org/10.1086/338782
- [27] Cama, Jehangir et al. “Single-cell microfluidics facilitates the rapid quantification of antibiotic accumulation in Gram-negative bacteria.” Lab on a chip vol. 20,15 (2020): 2765-2775. doi:10.1039/d0lc00242a
- [28] C. Schwall et al. “The Green Mother Machine: A microfluidics device for cyanobacteria full application” Synthetic biology in Cambridge. [Cited 1 March 2021]